Catalyst-Controlled C–C σ Bond Cleavages in Metal Halide-Catalyzed Cycloisomerization of 3-Acylcyclopropenes via a Formal 1,1-Halometalation Mechanism: Insights from Quantum Chemic...

2 AUTHORS, INCLUDING:

Genping Huang
Tianjin University

22 PUBLICATIONS **206** CITATIONS

Catalyst-Controlled C−C σ Bond Cleavages in Metal Halide-Catalyzed Cycloisomerization of 3-Acylcyclopropenes via a Formal 1,1-Halometalation Mechanism: Insights from Quantum Chemical Calculations

Genping Huang and Yuanzhi Xia*

College of Chemistry and Materials Engineering, Wenzhou University, Wenzhou 325035, P. R. China

S *Supporting Information*

ABSTRACT: The ring-opening cycloisomerization reactions of cyclopropenyl ketones developed by S. Ma et al. [*J. Am. Chem. Soc.* **2003**, *125*, 12386−12387] provided an efficient method for the constructions of trisubstituted furans in which an elegant control of the regiochemistry was achieved by using CuI or PdCl$_2$ catalyst. In the current report we aimed at uncovering the origin of the divergent regiochemistry of the reactions with different metal halide catalysts using quantum chemical calculations. By comparing the energies of all possible pathways, we found that a novel mechanism involving a formal 1,1-halometalation is the energetically most favorable one. In this pathway, an organometallic intermediate is involved from addition of the metal atom and the halide ligand to the same sp^2 carbon of the cyclopropene moiety by sequential 1,5-addition and 1,5-rearrangement steps, and the furan product is finally formed via an asynchronous intramolecular substitution/metal halide elimination process. The initial 1,5-addition was found to be the rate- and regiochemistry-determining step. The calculations reproduced well the experimentally observed selectivity. By analyzing the divergence of the Pd(II) and Cu(I) halides using the distortion/interaction model, it was found that the interaction energy plays a more important role in determining the selectivity. The strong π-affinity of PdCl$_2$ enables its strong coordination with the C^1=C^2 double bond in the TS, and the opening of the more substituted C^1−C^3 single bond is favored. On the other hand, the harder Lewis acid CuI is more sensitive to the steric effect and the opening of the less substituted C^2−C^3 single bond thus becomes predominant.

KEYWORDS: *3-acylcyclopropene, regioselective ring-opening, substituted furan, 1,1-halometalation, mechanistic study*
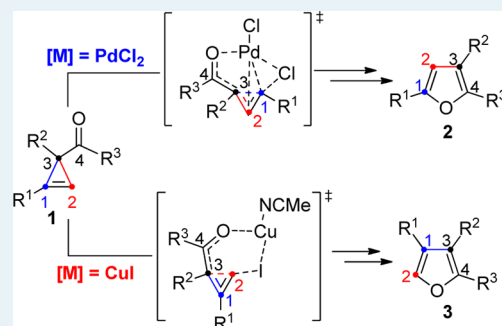
INTRODUCTION

Cyclopropenes are the smallest unsaturated carbocycles and represent one class of highly reactive species due to their highly strained structure.[1] As a result, these molecules readily undergo rearrangement or cycloaddition reaction that leads to relief of the ring strain.[2] With the development of efficient methods toward facile preparation of cyclopropenes, they are widely used as versatile building blocks for the construction of complex organic molecules.[3] While the rearrangements of cyclopropenes under thermal and photochemical conditions were the topic of numerous studies,[4] considerable attention has been paid to their isomerization reactions under transition metal catalysis in recent years, and facile constructions of carbo- and heterocycles by ring-opening reaction of cyclopropene derivatives have been extensively studied.[5]

Due to enhanced reactivity of both the C−C σ and π bonds in cyclopropenes,[1] generally three different types of organo-metallic intermediates (**A**, **B**, and **C**) could be possibly formed in transition metal-catalyzed reactions of cyclopropenes (Scheme 1). Intermediate **A** is a metal-substituted cyclopropane which could result from the addition of a metal and an anionic ligand to the double bond of the cyclopropene (Path a).[6] Such

Scheme 1. Typical Pathways for the Activation of Cyclopropene by Transition Metals
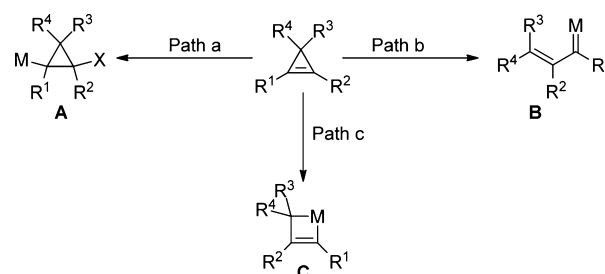
a mechanism has been widely employed for the functionalization of unsaturated molecules via hydrometalation, halometalation, carbometalation, and other related processes.[7] With the development of carbophilic noble metal catalysis in recent years,[8] the carbenoid **B** has been found to be a key intermediate

in the ring-opening transformations of cyclopropene under gold and platinum catalysis, resulting from the electrophilic activation of the C=C double bond (Path b).[9] Besides these processes, the oxidative addition with the insertion of a metal into the C−C single bond of cyclopropene to form a 4-membered ring intermediate **C** is commonly proposed for reactions involving transition metal catalysts of relatively low oxidation state (Path c).[10]

As results of different modes of activation based on transition metal catalysis, interesting issues of selectivity and reactivity were observed in ring-opening reactions of cyclopropenes, which are usually dependent on the substitution pattern and the reaction condition.[11] Thus, transformations based on selective C−C σ bond cleavage of cyclopropene derivatives are of great synthetic and mechanistic interests when the C=C double bond is unsymmetrically substituted.[12] To this end, notable catalyst-controlled C−C σ bond cleavages were discovered by S. Ma and co-workers in the metal halide-catalyzed rearrangements of 3-acylcyclopropenes (Scheme 2),[13] from which the

Scheme 2. Catalyst-Dependent Regioselectivity in the Metal Halide-Catalyzed Ring-Opening Cycloisomerization Reactions of Cyclopropenyl Ketones and Proposed Mechanism by S. Ma et al.[13]
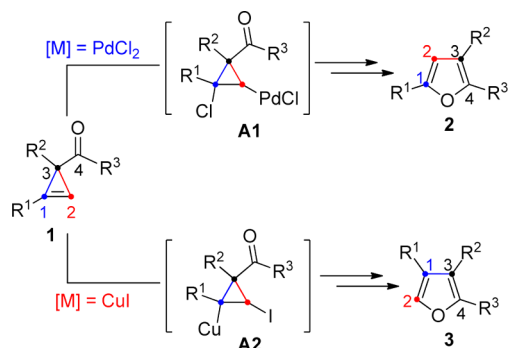

2,3,5- or 2,3,4-trisubstituted furans were obtained selectively when changing the catalyst from PdCl₂ to CuI.[14] This methodology is alternative to a previous report by Padwa et al.,[15] who found that the regioselectivity in the formations of substituted furans from 3-acylcyclopropenes could be well controlled by the oxidation state of the Rh catalyst, albeit only very limited examples were presented (eq 1).[16] In 2007, a complementary work on the rearrangements of 3-iminocyclo-propenes into fused pyrrole derivatives under the catalysis of RhCl(PPh₃)₃ or CuI was reported by the Gevorgyan group.[17] Consistently, the regiochemistry is also catalyst-dependent and the selective cleavage of the less substituted C−C single bond of the cyclopropene was observed when CuI was used as the catalyst (eq 2). In 2010, the S. Ma group reported the ring-expansion of cyclopropenyl carboxylates to form 1-alkoxyfurans (eq 3),[18] which were obtained in a regiodivergent fashion by change of the metal catalyst. Very recently, the catalyst-controlled site-selective ring-opening of chroman-4-one motif containing cyclopropenes was reported by the B. Ma group (eq 4).[19] These elegant works demonstrate the long-lasting interest of researchers in both the site selective C−C σ bond cleavage of cyclopropenes and the controllable synthesis of polysubstituted furans[20] and pyrroles,[21] yet very little attention has been paid to the detailed mechanism of related reactions. A regiodivergent 1,2-halometalation step (forming **A1** and **A2**, Scheme 2) was
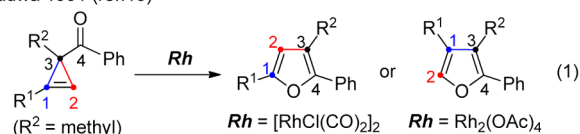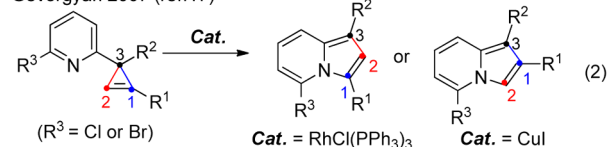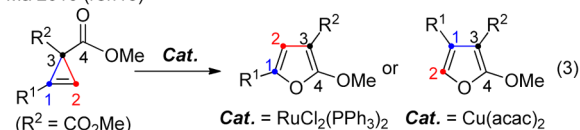

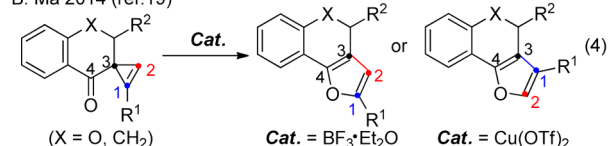proposed to be responsible for the different selectivity in S. Ma's reactions using different metal halides,[13,20] to the best of our knowledge, however, there is no literature precedent available for an explicit understanding of the intriguing metal-dependent selectivity in the reactions concerned.[22]

In the current report, we carried out quantum chemical calculations at the CCSD(T)//B3LYP level to study the catalyst-dependent regiochemistry in the PdCl₂- and CuI-catalyzed ring-opening cycloisomerization reactions of cyclo-propenyl ketones in Scheme 2.[13] Instead of undergoing the previously known processes for ring-opening of cyclopropenes, the results showed that a novel mechanism involving a formal 1,1-halometalation process is the most favorable and agrees well with the experimental observations. The divergence between Pd(II) and Cu(I) halides in this unprecedented process was analyzed theoretically.[23,24]

■ COMPUTATIONAL DETAILS

All calculations were carried out with the Gaussian 09 suite of computational programs.[25] The geometries of all stationary points were optimized at the DFT level using the B3LYP functional.[26] The 6-31+G(d) basis set[27] was applied for all atoms except for Pd, Cu, and I, which were described by the SDD basis set.[28] Frequencies were analytically computed at the same level of theory to obtain the gas phase free energies and to confirm whether the structures are minima (no imaginary frequency) or transition states (only one imaginary frequency). All transition state structures were confirmed to connect the proposed reactants and products by intrinsic reaction coordinate (IRC) calculations.[29] The effect of solvent was examined by performing single-point self-consistent reaction field (SCRF) calculations based on the polarizable continuum model (PCM) for gas-phase optimized structures.[30] Acetonitrile (ε = 35.688) and dichloro-methane (ε = 8.930) were respectively used as the solvents in CuI- and PdCl₂-catalyzed reactions, corresponding to original experimental conditions,[13] and the atomic radii used for the PCM calculations were specified using the UFF keyword. To obtain more accurate predictions, all energies were corrected by single-point calculations at the CCSD(T) level with a larger basis set combined by def2-TZVPPD for Pd, Cu, and I and 6-31+G(d,p) for all other atoms. The final energies (kcal/mol) reported in the manuscript are relative free energies including electronic energy from the CCSD(T) calculation,

thermal correction at the B3LYP level, and solvation correction with PCM model.

While the predictions from high level CCSD(T) calculations are in good agreement with the experiments, consistent results were also obtained from the B3LYP calculations as given in the Supporting Information. This validated the B3LYP functional as a reliable method for mechanistic investigation of related reactions.

In original experiments by S. Ma et al. despite the reacting carbonyl functionality, another acyl group was generally contained at C^3 of the cyclopropene precursors.[13] Hence, the 3,3-diacetyl-1-methylcyclopropene (**1a**, Scheme 3) was used as a model substrate in our

Scheme 3. Formation of the Reactant Complexes
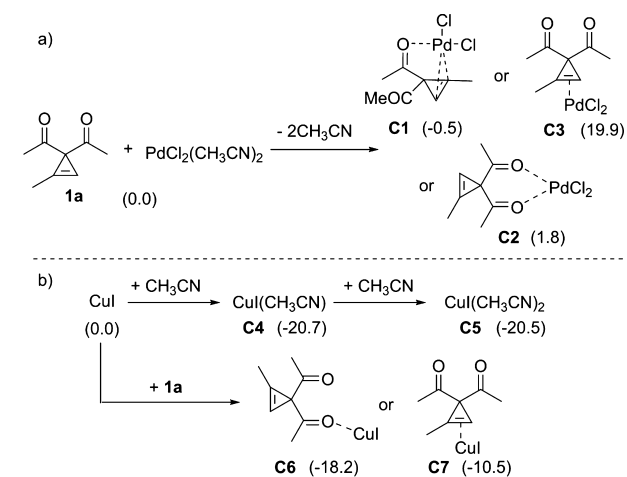
computations. Both $PdCl_2$ and $PdCl_2(CH_3CN)_2$ were effective catalysts for the selective opening of the C^1-C^3 single bond of **1** (Scheme 2), indicating the possible involvement of CH_3CN as a neutral ligand does not influence the catalytic activity of the Pd complex. Consistently, the results in Scheme 3a show the displacement of the two acetonitrile ligands of $PdCl_2(CH_3CN)_2$ with **1a** to form chelate complex **C1**, in which the Pd atom is coordinated by both the carbonyl oxygen and the $C^1=C^2$ double bond, is an almost energetically neutral process, while the formations of complexes **C2** and **C3** are endergonic. The formation of **C1** from the ligand-free $PdCl_2$ and **1a** is much more favorable with an exergonicity of 30.1 kcal/mol. As all CuI-catalyzed reactions were carried out in the acetonitrile solution, the possible complexation of CuI with the solvent was considered. It was found the formations of solvated complexes **C4** and **C5** (eq 2) are more favorable than the formations of reactant complexes **C6** and **C7** (eq 3). Calculations indicated only one oxygen atom is coordinated to the Cu atom in **C6** and no complex could be formed from **C4** and **1a**. Accordingly, the reactant complex **C1** was established as the starting point of the $PdCl_2$-catalyzed reaction whereas separated **C4** and **1a** were used for the simulation of the CuI-catalyzed reaction in acetonitrile.
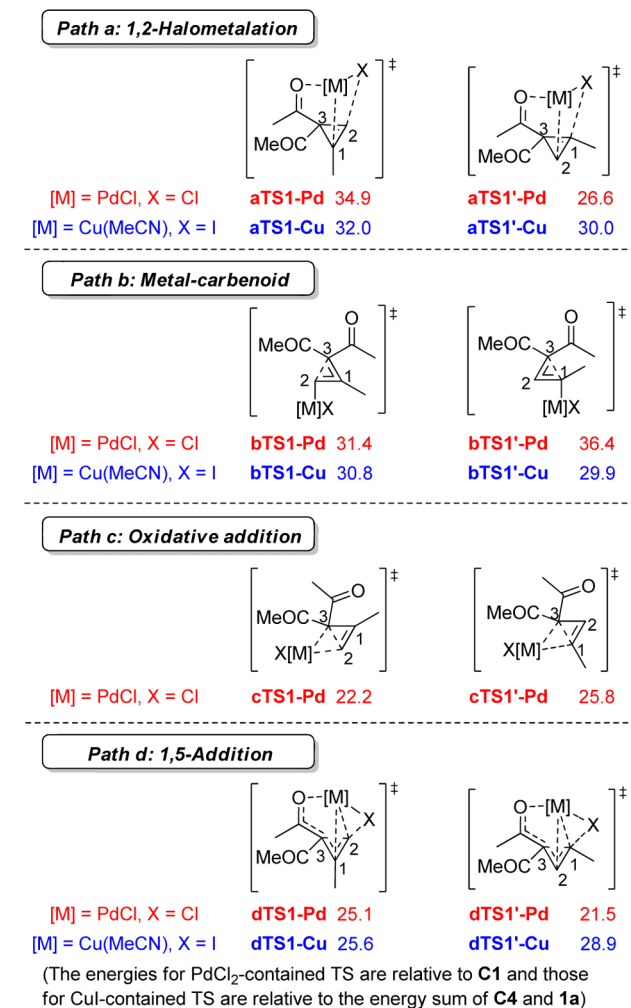
We included one acetonitrile solvent as a ligand to CuI not only because **C4** is the most stable complex in Scheme 3b, but also lower energies were calculated for the TS when an explicit solvent is contained. On the other hand, if one CH_3CN ligand is involved in the $PdCl_2(CH_3CN)_2$-catalyzed reaction, no chelate complex like **C1** could be formed due to the coordination saturation of the Pd center and a different mechanism was suggested. The ligand free CuI-catalyzed and the CH_3CN-contained $PdCl_2$-catalyzed reactions of **1a** are given in the Supporting Information.

■ RESULTS AND DISCUSSION

Possible Initiations. As shown in Scheme 1, different types of activation are possible for the ring-opening of cyclopropenes. To disclose which pathway is the most favorable for the Pd(II) and Cu(I)-catalyzed reactions of **1a**, the relative energies for

transition states (TSs) of all possible initiations were compared in Scheme 4. First of all, the originally proposed 1,2-

Scheme 4. Relative Energies (kcal/mol) for the Key TS in Possible Pathways

(The energies for $PdCl_2$-contained TS are relative to **C1** and those for CuI-contained TS are relative to the energy sum of **C4** and **1a**)

halometalation mechanism (Path a) was evaluated. Despite higher activation energies were required for this pathway in comparison with some of other possibilities (Scheme 4), the additions of both Pd and Cu atoms to the less substituted sp^2 carbon (C^2) were found to be more favorable, as the **aTS1'-Pd** is 8.3 kcal/mol lower in energy than **aTS1-Pd** and the **aTS1'-Cu** is 2.0 kcal/mol lower than **aTS1-Cu**. The unfavorable reactions via **aTS1** could be attributed to the steric effect of the methyl substituent at C^1, which prevents the addition of the metal moiety to this carbon. Thus, the same regiochemistry will be expected for both Pd- and Cu-catalyzed reactions if the 1,2-halometalation is the selectivity-determining step.

In Path b, the metal-carbenoids could be formed via **bTS1** and **bTS1'** as results of the electrophilic activation of the $C^1=C^2$ double bond by the metal catalyst.[9] This pathway could be excluded due to the relatively higher activation barriers. Furthermore, the predicted selectivity is just opposite to that observed in both reactions. Accordingly, when the $PdCl_2$ is involved, the ring-opening of cyclopropene **1a** occurs more favorably via **bTS1-Pd** to cleave the less substituted C^2-C^3 single bond. This is 5.0 kcal/mol lower in energy than that via **bTS1'-Pd**. On the other hand, the **bTS1'-Cu** is slightly lower in
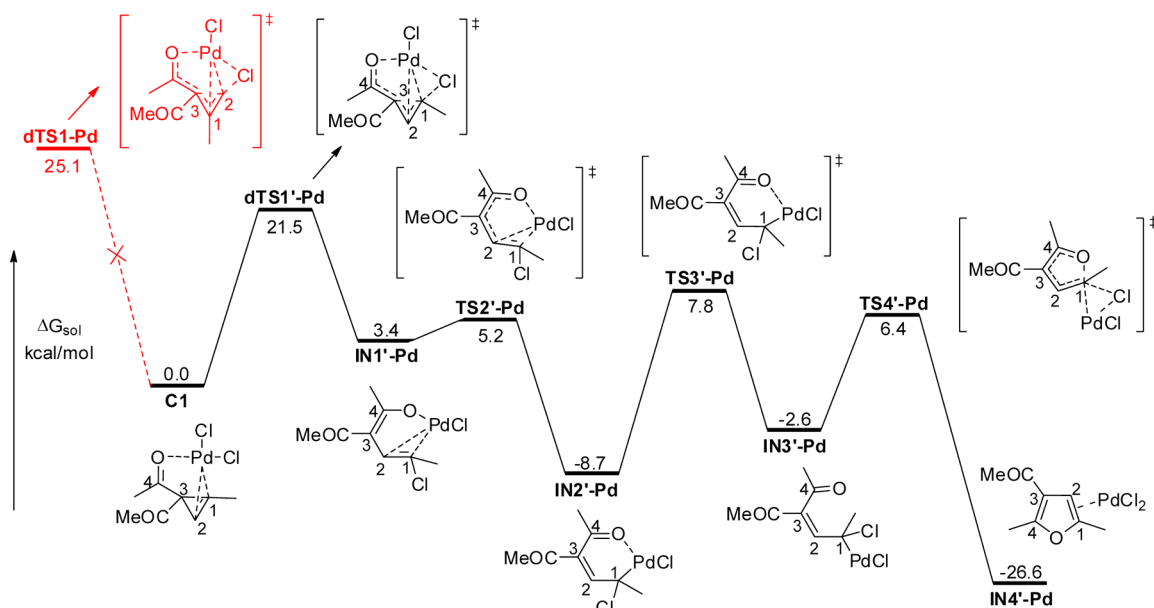
Figure 1. Full energy profile for the PdCl$_2$-catalyzed reaction via the 1,5-addition pathway.
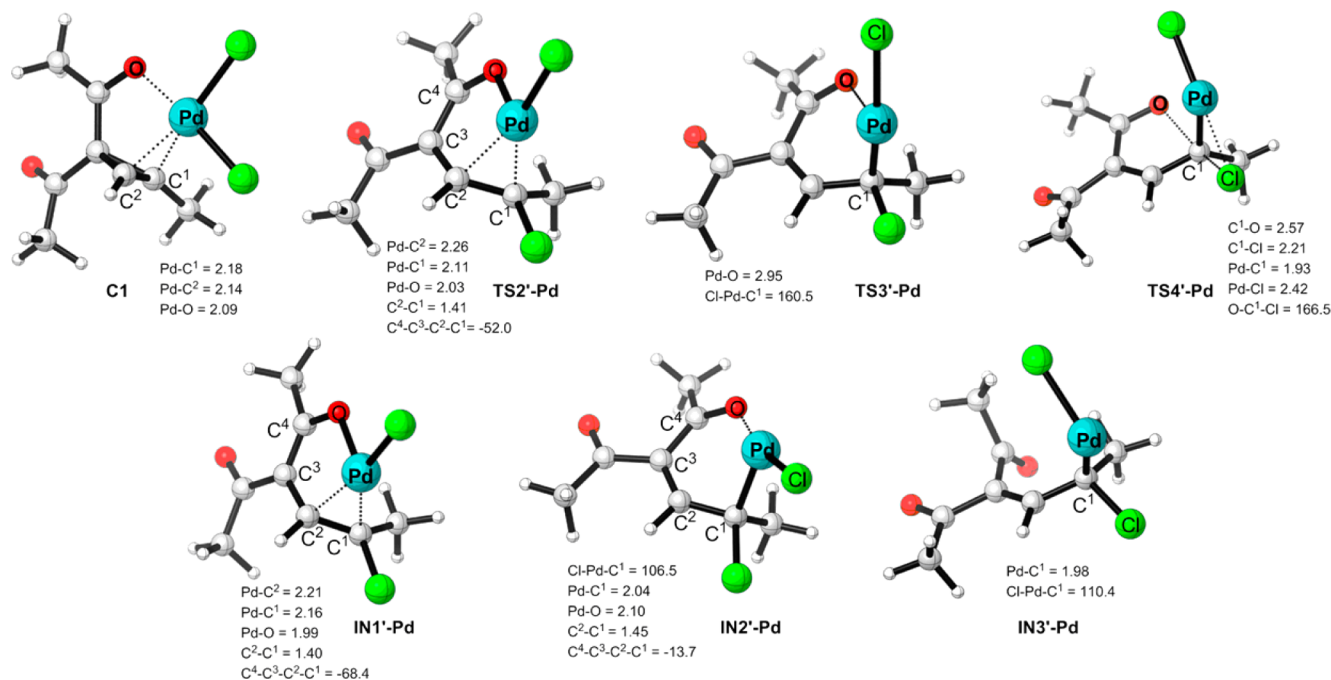

Figure 2. Geometries for selected stationary points in the PdCl$_2$-catalyzed reaction (distances and angles are in angstroms and degrees, respectively).

energy (0.9 kcal/mol) than **bTS1-Cu**, suggesting cleavage of the C^1−C^3 single bond is more preferred in case of CuI catalyst. The difference between PdCl$_2$ and CuI in this process was analyzed in the Supporting Information.

Although the oxidative addition of organic electrophile to PdCl$_2$ is quite rare (Path c), the insertions of PdCl$_2$ into the C^2−C^3 and C^1−C^3 single bonds of **1a** were found to be possible via **cTS1-Pd** and **cTS1′-Pd** with activation barriers of 22.2 and 25.8 kcal/mol, respectively. Despite the relatively lower energy barrier, it seems to contradict with the experimentally observed selectivity since **cTS1-Pd** is 3.6 kcal/mol more favorable than **cTS1′-Pd**. In fact, a detailed analysis of the full potential energy surface in the coming subsection shows the oxidative additions via **cTS1-Pd** and **cTS1′-Pd** are

reversible and thus are not the selectivity-determining step in Path c. Calculations to uncover the energies for oxidative addition of **1a** to CuI or **C4** were also conducted, however, all attempts to locate the TS similar to **cTS1-Pd** and **cTS1′-Pd** failed.

Besides the above processes for the activation of **1a** with PdCl$_2$ and CuI, a new pathway initiated by 1,5-addition of the metal halide to **1a** was disclosed by calculations (Path d). By passing through transition states **dTS1** and **dTS1′**, the metal atom is adding to the carbonyl oxygen while the halide ligand is adding to C^2 and C^1, respectively, with concurrent cleavage of the C^2−C^3 and C^1−C^3 bonds, generating the metal enolates as intermediates. Albeit the details for the following steps in Path d remain undisclosed, interestingly, for each metal halide, the

required activation free energy is the lowest among all possible pathways given in Scheme 4 and the predicted regioselectivity agrees well with that in experiments (Scheme 2).[13] Therefore, an in-depth analysis of this new approach for ring-opening of 3-acylcyclopropene and the key factors governing the regiochemistry of the PdCl$_2$- and CuI-catalyzed reactions will be presented.

Details for the Pd(II)-Catalyzed Reaction. According to the above results, the initiation via **dTS1′-Pd** has the lowest relative free energy of 21.5 kcal/mol among all possible TS when PdCl$_2$ is the catalyst. The full potential energy surface is depicted in Figure 1 to show how the 2,3,5-trisubstituted furan is finally formed through this pathway. Except for the structure of **dTS1′-Pd**, which will be compared more closely later with **dTS1-Pd** and with the CuI-involved counterparts to highlight the key difference between the reactions, the geometric structures for all other TS and intermediates in this mechanism are given in Figure 2.

From Figure 1, it can be concluded that the first step of the 1,5-addition is the rate- and selectivity-determining step of the whole reaction and will lead to product complex **IN4′-Pd** irreversibly, as all other transition states are lower in energies than **dTS1′-Pd**. This further confirms that the 1,2-halometalation in Path a is not possible. Upon the 1,5-addition, the opening of the C^1−C^3 σ bond is achieved and the palladium 1,3-dienolate **IN1′-Pd** is formed endergonically by 3.4 kcal/mol, in which the Pd atom is coordinated strongly by the chloro-substituted C^1=C^2 π bond (Pd−O = 1.99, Pd−C^1 = 2.16, and Pd−C^2 = 2.21 Å, Figure 2). In the following step, isomerization of **IN1′-Pd** via a 1,5-Pd migration occurs facilely via **TS2′-Pd** (Pd−O = 2.03, Pd−C^1 = 2.11, and Pd−C^2 = 2.26 Å) with a barrier of less than 2.0 kcal/mol. The easiness for the isomerization of **IN1′-Pd** is understandable as only marginal structural change is required to reach the TS. Also, this step is favored due to the thermodynamic preference of alkyl palladium intermediate **IN2′-Pd**, which is 12.1 kcal/mol more stable than the enolate form and is the global minimum of the whole potential energy surface. Thus, the **IN2′-Pd** could be viewed as the result of a formal 1,1-chloropalladation reaction of **1a** with PdCl$_2$, from which both Pd and Cl atoms of the catalyst moiety are σ-bonded to C^1 of the 3-acylcyclopropene moiety.

In **IN2′-Pd**, the Pd atom is still coordinated by the carbonyl oxygen. Prior to the formation of the C^1−O σ bond that required in the furan product, this intermediate should be first transformed to its conformational isomer **IN3′-Pd** via dissociation of the Pd⋯O interaction, which is realized by passing through **TS3′-Pd** with an activation barrier of 16.5 kcal/mol. Due to the absence of the Pd⋯O coordinative bond, **IN3′-Pd** is 6.1 kcal/mol higher in energy than **IN2′-Pd** and now the Pd atom is associated with the chloride on C^1 (Pd−Cl = 2.51 Å). From **IN3′-Pd**, the final intramolecular cyclization to form the aromatic heterocycle occurs via **TS4′-Pd** with an activation barrier of 9.0 kcal/mol. The cyclization via **TS4′-Pd** could be described as a nucleophilic substitution process as the TS adopts a trigonal bipyramidal geometry in which the attacking of the oxygen atom to C^1 occurs from the backside of the chloride atom (O−C^1 = 2.57, Cl−C^1 = 2.21 Å, and O−C^1−Cl = 166.5°). The Pd−C^1 distance in **TS4′-Pd** (1.93 Å) is even slightly shorter than that in the preceding intermediate **IN3′-Pd** (1.98 Å); however, the elimination of PdCl$_2$ occurs asynchronously with the leaving of the chloride atom from C^1, affording **IN4′-Pd**, the π complex of 2,3,5-trisubstituted

furan product and PdCl$_2$, exergonically. The results above disclosed how the 2,3,5-trisubstituted furan is formed in the PdCl$_2$-catalyzed reaction from the 1,5-addition via **dTS1′-Pd**. As expected, following a similar potential energy surface, the regioisomeric 1,5-addition via **dTS1-Pd** will open C^2−C^3 σ bond and lead irreversibly to a 2,3,4-trisubstituted furan product (see the Supporting Information for details). The energy for the latter TS is 3.6 kcal/mol higher than that of the former one (Figure 1), in good agreement with the experiments in which the 2,3,5-trisubstituted furan were formed predominantly. However, the calculated energy for the oxidative addition via **cTS1-Pd** for opening the C^1−C^3 σ bond is only 0.7 kcal/mol higher than **dTS1′-Pd** but 2.9 kcal/mol lower than **dTS1-Pd**, suggesting Path c may be a more preferred pathway than Path d (via **dTS1-Pd**) to generate the 2,3,4-trisubstituted furan byproduct. To make clear how the very small amount of 2,3,4-trisubstituted furan was formed in the PdCl$_2$-catalyzed reactions, the full potential energy surface for the oxidative addition pathways initiated by **cTS1-Pd** and **cTS1′-Pd** is shown in Figure 3.
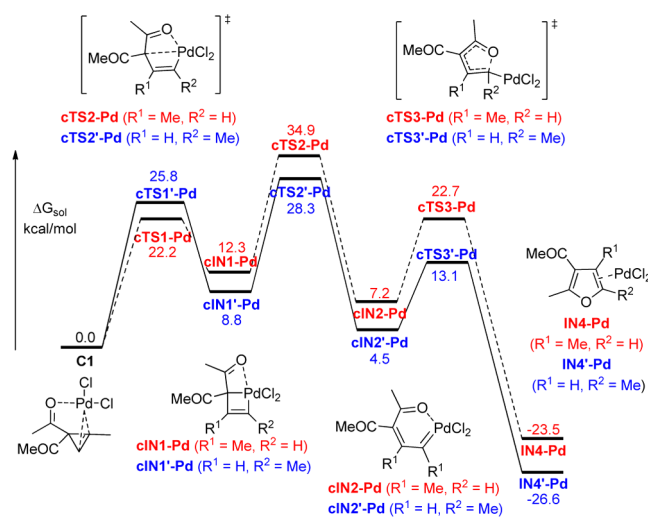

Figure 3. Full energy profile for the PdCl$_2$-catalyzed reaction via Path c.

In Path c, both the insertions of the Pd atom into C^1−C^3 and C^2−C^3 σ bonds via **cTS1-Pd** and **cTS1′-Pd**, respectively, are reversible, with the former TS being lower in energy by 3.6 kcal/mol. As shown by the geometries depicted in the Supporting Information, the carbonyl oxygen is coordinated to the Pd atom in both TS and in the generated four-membered palladacycle intermediates **cIN1-Pd** and **cIN1′-Pd**. Then the reactions undergo the cleavage of the Pd−C^3 σ bonds via **cTS2-Pd** and **cTS2′-Pd** with relative energies of 34.9 and 28.3 kcal/mol, respectively, which are the highest values in both pathways. As the rearrangement of the four-membered ring organometallic intermediate is the regiochemistry-determining step in Path c, the pathway initiated by **cTS1-Pd** for opening of the C^1−C^3 σ bond becomes unfavorable. Therefore, the generation of carbenoid intermediate **cIN1′-Pd** from **cTS2′-Pd** is more favorable than **cIN1-Pd**, and finally, the formation of complex **IN4′-Pd** will be predominant by a facile ring-closure via **c-TS3′-Pd**. Thus, the PdCl$_2$-catalyzed oxidative addition pathway may actually lead to the main product of 2,3,5-trisubstituted furan, but it is kinetically less favorable than Path d as **cTS2′-Pd** is 6.8 kcal/mol higher in energy than **dTS1′-Pd**.
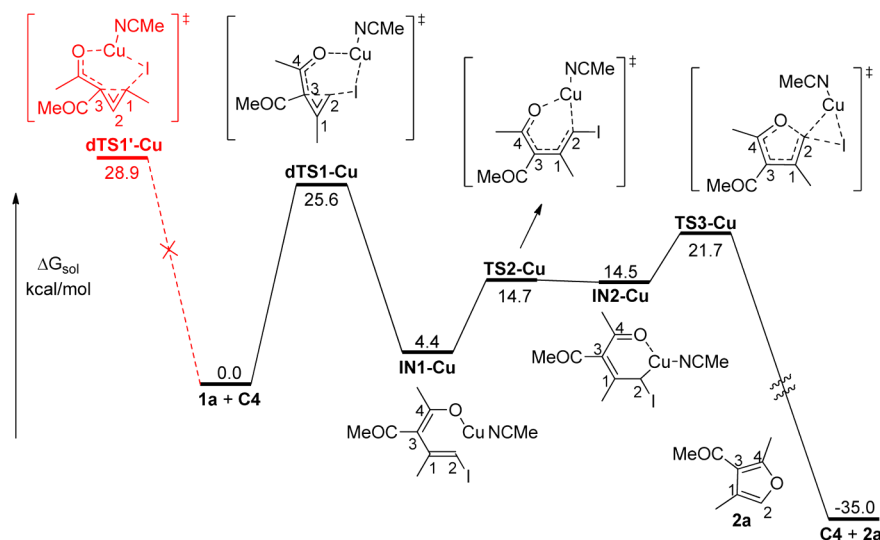
Figure 4. Full energy profile for the CuI-catalyzed reaction via the 1,5-addition pathway.

This also confirms that the 2,3,4-trisubstituted furan byproduct is formed from the 1,5-addition via **dTS1-Pd**.

Details for the Cu(I)-Catalyzed Reaction. Although the TS for the oxidative addition of **1a** to CuI was not located, Path c was excluded by calculations of the energies from the possible intermediates of the oxidative addition, which showed the cleavage of the Cu−C^3 bonds (similar to **cTS2-Pd** and **cTS2'-Pd**) require relatively high energies (see the Supporting Information for details). As **dTS1-Cu** in Path d has the lowest energy among all possible initiations in Scheme 4 when monoacetonitrile-ligated complex **C4** is the catalyst, the detailed potential energy surface for this pathway is given in Figure 4 and selected geometric structures are depicted in Figure 5.

It was found that the CuI-catalyzed reaction follows a similar mechanism as that for the PdCl$_2$-catalyzed one. The 1,5-

addition via **dTS1-Cu** has a highest energy value of 25.6 kcal/mol in Figure 4 and leads to Cu(I) enolate **IN1-Cu** slight endergonically. Distinguished from the Pd(II) enolate **IN2'-Pd**, only very week interaction between Cu and C^1═C^2 π bond was calculated for **IN1-Cu** (Cu−O = 1.84, Cu−C^1 = 2.87, and Cu−C^2 = 3.06 Å), demonstrating the dramatic difference in electronic properties between Pd(II) and Cu(I). In a following step, the 1,5-rearrangement of **IN1-Cu** is realized via **TS2-Cu** (Cu−O = 2.08, Cu−C^1 = 2.69, and Cu−C^2 = 2.05 Å), resulting in the alkyl copper intermediate **IN2-Cu** with an activation barrier of 10.3 kcal/mol. Although is still facile, this step requires a much higher barrier than the rearrangement of its counterpart with PdCl$_2$ (**IN1'-Pd**), because the formation of **IN2-Cu** is an endergonic process. In this latter intermediate the Cu···O coordinative bond is at a distance of 2.21 Å and no further rearrangement is required before the cyclization/substitution via **TS3-Cu**. This final C−O bond formation step requires an overall barrier of 17.3 kcal/mol from **IN1-Cu** and gives rise to separated **C4** and 2,3,4-trisubstituted furan product **2a** highly exergonically.

Similarly, the 2,3,5-trisubstituted furan product **3a** could be formed from Path d through the 1,5-addition via regioisomer **dTS1'-Cu**. This is 3.3 kcal/mol higher in energy than **dTS1-Cu** and thus is kinetically unfavorable in competition with the pathway shown in Figure 4, accounting for the highly regioselective cycloisomerization of **1a** to 2,3,4-trisubstituted furan under the catalysis of CuI in acetonitrile.

Divergence between the Two Metal Halides. Having established the Path d as the lowest energy pathway and shown how the 2,3,5- and 2,3,4-trisubstituted furans were respectively formed in the PdCl$_2$- and CuI-catalyzed reactions of **1a**, we next carried out a closer examination of the relationship between structure and reactivity in the regioselectivity-determining 1,5-addition step to better understand the computational results. As shown by the geometric structures of the key TS in Figure 6, all these 1,5-additions resemble the bimolecular nucleophilic substitution processes, in which the addition of the halogen atom to C^1 (or C^2) and the opening of the C^1−C^3 (or C^2−C^3) σ bond occur concertedly.[31] A notable difference between TS of different metal catalysts is that the Pd(II) has strong interaction with the C^1═C^2 π bond in the process of 1,5-addition while such interaction is relatively weak in cases of
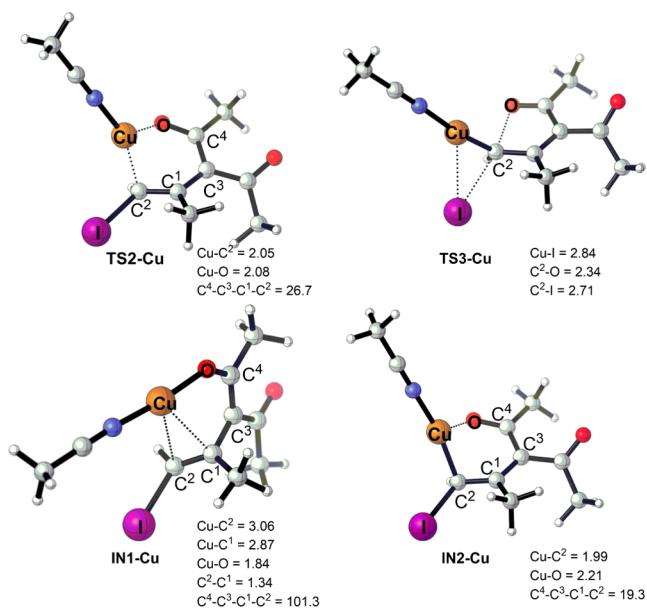

Figure 5. Geometries for selected stationary points in the CuI-catalyzed reaction (distances and angles are in angstroms and degrees, respectively).
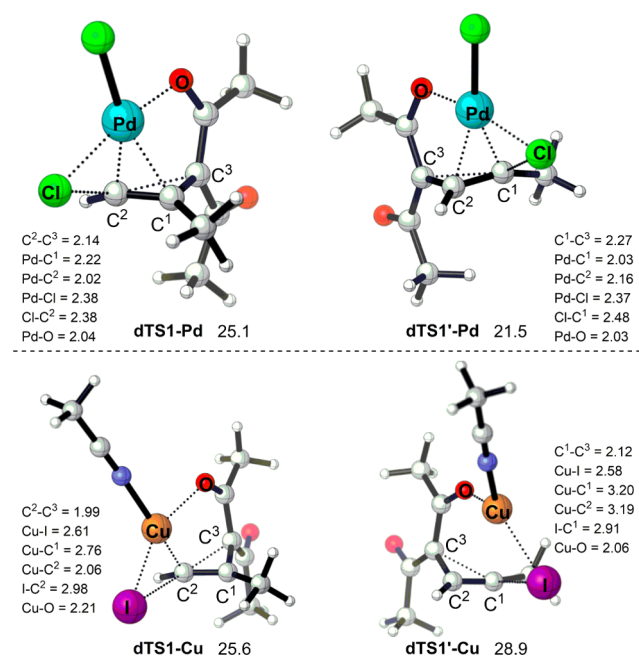
C²-C³ = 2.14
Pd-C¹ = 2.22
Pd-C² = 2.02
Pd-Cl = 2.38
Cl-C² = 2.38
Pd-O = 2.04

dTS1-Pd 25.1

C¹-C³ = 2.27
Pd-C¹ = 2.03
Pd-C² = 2.16
Pd-Cl = 2.37
Cl-C¹ = 2.48
Pd-O = 2.03

dTS1′-Pd 21.5

C²-C³ = 1.99
Cu-I = 2.61
Cu-C¹ = 2.76
Cu-C² = 2.06
I-C² = 2.98
Cu-O = 2.21

dTS1-Cu 25.6

C¹-C³ = 2.12
Cu-I = 2.58
Cu-C¹ = 3.20
Cu-C² = 3.19
I-C¹ = 2.91
Cu-O = 2.06

dTS1′-Cu 28.9

Figure 6. Geometric structures for **dTS1-Pd**, **dTS1′-Pd**, **dTS1-Cu**, and **dTS1′-Pd** (selected distances are in angstroms).

Cu(I). For example, in **dTS1-Pd** the $Pd-C^1$ and $Pd-C^2$ distances are 2.22 and 2.02 Å, respectively, and in **dTS1′-Pd** these two distances are 2.03 and 2.16 Å, respectively. On the other hand, the Cu(I) only interacts unsymmetrically with the $C^1=C^2$ π bond in **dTS1-Cu** with the $Cu-C^1$ and $Cu-C^2$ distances being 2.76 and 2.06 Å, respectively, whereas in **dTS1′-Cu** almost no interaction was found ($Cu-C^1$ = 3.20 and $Cu-C^2$ = 3.19 Å). This difference in geometric structures demonstrates the stronger Lewis acidity and π-affinity of $PdCl_2$ than CuI,[32] especially when the latter catalyst is σ-coordinated by the CH_3CN solvent in reactions. The stronger Lewis acidity and π-affinity of $PdCl_2$ are also shown by the favorable formation of chelate complex **C1** over **C2** and **C3**, while the formation of π-complex **C7** from CuI and **1a** is the least favorable compared with the σ-complexes (Scheme 3). In addition, in the generated 1,3-dienolate intermediates from the 1,5-addition, the Pd atom is strongly associated with the $C^1=C^2$ π bond in **IN1′-Pd** but no such interaction was found for the CuI-containing counterpart **IN1-Cu** (or **IN1′-Cu**).

To gain more insights into the physical factors that control the activation barriers of the 1,5-addition processes, the distortion/interaction analysis of key transition states is given in Table 1. The distortion/interaction model[33] is also known as the activation-strain model,[34] which has been applied to explain the reactivities and selectivities in different systems including the transition metal catalysis.[33,34] In bimolecular reaction, the activation barrier ($\Delta E^{\ddagger}$) could be decomposed into two contributions, the distortion energy (ΔE_{dist}) which is the energy required to deform the reactants from their equilibrium

geometries to the geometries they adopt in the TS and the interaction energy (ΔE_{int}) which is the energy of interaction between the deformed fragments. Although the transformations from reactant complex **C1** is not a bimolecular reaction, the distortion/interaction model should be still applicable here to show the difference between **dTS1-Pd** and **dTS1′-Pd** by using complex **C1** as a reference, as suggested by Fernández and Bickelhaupt.[35] According to Table 1, the energies for distortion of the $PdCl_2$ moiety ($\Delta E_{dist}(MX_n)$) are quite close in **dTS1-Pd** and **dTS1′-Pd**, but the distortion energy of **1a** moiety ($\Delta E_{dist}(\mathbf{1a})$) is 7.2 kcal/mol higher in the latter case than in the former case. This is corresponding to the relatively longer breaking C^1-C^3 distance in **dTS1′-Pd** (2.27 Å) than the breaking C^2-C^3 distance in **dTS1-Pd** (2.14 Å). Besides, the stronger steric effect arising from the Pd moiety and the methyl on C^1 also contributes to greater distortion of **1a** in **dTS1′-Pd**. Thus, the total distortion energy required for **dTS1-Pd** is 6.7 kcal/mol lower than **dTS1′-Pd**. However, the latter TS is favored as its interaction energy is 9.0 kcal/mol lower than the former one, implying the stronger coordination between $PdCl_2$ and **1a** in **dTS1′-Pd** than in **dTS1-Pd** is the major factor that results in the observed selectivity. This conclusion is supported by the Wiberg bond index calculations, which showed the sum of bond orders for the $Pd-O$, $Pd-C^1$, and $Pd-C^2$ distances in **dTS1′-Pd** is 1.30, being slightly greater than the value of 1.22 in **dTS1-Pd**.

While the $PdCl_2$-catalyzed 1,5-addition is explained by the distortion/interaction model, it should be noted that the favorable opening of the more substituted C^1-C^3 σ bond via **dTS1′-Pd** is consistent with the bond strength. The calculated bond dissociation enthalpy for the C^2-C^3 σ bond in **1a** is 11.2 kcal/mol higher than that for the C^1-C^3 σ bond,[36] indicating the more substituted C^1-C^3 σ bond is intrinsically more reactive.

In case of CuI, the catalyst moiety is more distorted (by 5.4 kcal/mol) in **dTS1-Cu** than in **dTS1′-Cu**, in line with the slightly longer $Cu-I$ distance (2.61 vs 2.58 Å) and the smaller $N-Cu-I$ angle (112.5° vs 128.9°) in the former TS. On the other hand, the **1a** is more distorted in **dTS1′-Cu** with the distortion energy being 2.9 kcal/mol higher than that in **dTS1-Cu**, due to the longer opening C^1-C^3 distance (2.12 vs 1.99 Å) and the steric effect between the iodide atom and the C^1 methyl group in the former TS. In all, the ΔE_{dist} for **dTS1-Cu** is 2.5 kcal/mol higher than **dTS1′-Cu**. Similar to that found in the $PdCl_2$ case, the interaction energy plays a more predominant role in determining the selectivity and the **dTS1-Cu** is finally more preferred with more energy compensation from the stronger catalyst-substrate interaction. The calculated bond orders for the $Cu-O$, $Cu-C^1$, and $Cu-C^2$ distances in **dTS1-Cu** are 0.19, 0.10, and 0.28, respectively, while these values are 0.22, 0.02, and 0.01 in **dTS1′-Cu**. The selectivity is also in accordance with the steric effect that the less substituted C^2 atom is more accessible for the addition of the iodide atom.

■ CONCLUSIONS

In summary, the mechanism for regiochemical-controlled cycloisomerization of cyclopropenyl ketones was studied by quantum chemical calculations and insights into the difference between the catalysis of Pd(II) and Cu(I) halides were provided. The results show that the previously known processes for ring-opening of the cyclopropenes are higher in activation energies and do not agree with observed selectivity. Instead, a novel 1,1-halometalation mechanism initiated by the 1,5-

Table 1. Distortion/Interaction Analysis of Key TS

TS	$\Delta E^{\ddagger}$	ΔE_{dist} (MX_n)	ΔE_{dist} (**1a**)	ΔE_{dist}	ΔE_{int}
dTS1-Pd	23.9	6.4	37.6	44.0	−20.1
dTS1′-Pd	21.6	5.9	44.8	50.7	−29.1
dTS1-Cu	10.9	16.5	28.2	44.7	−33.8
dTS1′-Cu	12.9	11.1	31.1	42.2	−29.3

addition was uncovered as the lowest energy pathway. This pathway leads to an organometallic intermediate with both the metal atom and the halide ligand being added to the same sp^2 carbon of the cyclopropene moiety from sequential 1,5-addition and 1,5-rearrangement steps, and finally, the furan product is formed via an asynchronous intramolecular nucleophilic substitution/metal halide elimination process.

The full potential energy surfaces indicated the initial 1,5-addition is the regiochemistry-determining step. In this process, the stronger π-affinity of $PdCl_2$ enables its strong coordination with the $C^1{=}C^2$ double bond in the TS, and the opening of the more substituted C^1-C^3 single bond is favored. On the other hand, the harder Lewis acid CuI is more sensitive to the steric effect and thus the opening of the less substituted C^2-C^3 becomes predominant. Analysis of the key TS by the distortion/interaction model indicated the interaction between the distorted catalyst and substrate fragments plays a major role in determining the site of the ring-opening. The results here provided a full understanding of the intriguing results by S. Ma et al.[13] and should have mechanistic implications in related reactions.[14,15,17–19,31]

■ ASSOCIATED CONTENT

ⓢ Supporting Information

The following file is available free of charge on the ACS Publications website at DOI: 10.1021/cs501738p.

Additional results and discussion (PDF)

■ AUTHOR INFORMATION

Corresponding Author
*E-mail: xyz@wzu.edu.cn.

Notes
The authors declare no competing financial interest.

■ ACKNOWLEDGMENTS

■ REFERENCES

(1) (a) Fattahi, A.; McCarthy, R. E.; Ahmad, M. R.; Kass, S. R. *J. Am. Chem. Soc.* **2003**, *125*, 11746–11750. (b) Khoury, P. R.; Goddard, J. D.; Tam, W. *Tetrahedron* **2004**, *60*, 8103–8112. (c) Bach, R. D.; Dmitrenko, O. *J. Am. Chem. Soc.* **2006**, *128*, 4598–4611. (d) Tian, Z.; Lis, L.; Kass, S. R. *J. Org. Chem.* **2013**, *78*, 12650–12653.

(2) For recent theoretical studies on the unique reactivity of cyclopropenes in cycloaddition reactions, see: (a) Hong, X.; Liang, Y.; Griffith, A. K.; Lambert, T. H.; Houk, K. N. *Chem. Sci.* **2014**, *5*, 471–475. (b) Yang, J.; Liang, Y.; Seckute, J.; Houk, K. N.; Devaraj, N. K. *Chem.—Eur. J.* **2014**, *20*, 3365–3375. (c) Liu, F.; Paton, R. S.; Kim, S.; Liang, Y.; Houk, K. N. *J. Am. Chem. Soc.* **2013**, *135*, 15642–15649. (d) Kamber, D. N.; Nazarova, L. A.; Liang, Y.; Lopez, S. A.; Patterson, D. M.; Shih, H.-W.; Houk, K. N.; Prescher, J. A. *J. Am. Chem. Soc.* **2013**, *135*, 13680–13683.

(3) (a) Binger, P.; Büch, H. M. Cyclopropenes and methylenecyclopropanes as multifunctional reagents in transition metal catalyzed reactions. *Small Ring Compounds in Organic Synthesis II*; Topics in Current Chemistry; Springer, 1987; Vol. 135, pp 77–151. (b) Nakamura, M.; Isobe, H.; Nakamura, E. *Chem. Rev.* **2003**, *103*, 1295–1326. (c) Fox, J. M.; Yan, N. *Curr. Org. Chem.* **2005**, *9*, 719–

732. (d) Marek, I.; Simman, S.; Masarwa, A. *Angew. Chem., Int. Ed.* **2007**, *46*, 7364–7376.

(4) (a) Baird, M. S. *Chem. Rev.* **2003**, *103*, 1271–1294. (b) Walsh, R. *Chem. Soc. Rev.* **2005**, *34*, 714–732. (c) Padwa, A.; Krumpe, K. E.; Terry, L. W.; Wannamaker, M. W. *J. Org. Chem.* **1989**, *54*, 1635–1642. (d) Padwa, A.; Chou, C. S.; Rosenthal, R. J.; Terry, L. W. *J. Org. Chem.* **1988**, *53*, 4193–4201. (e) Padwa, A.; Kennedy, G. D. *J. Org. Chem.* **1984**, *49*, 4344–4352.

(5) (a) Rubin, M.; Rubina, M.; Gevorgyan, V. *Synthesis* **2006**, *8*, 1221–1245. (b) Rubin, M.; Rubina, M.; Gevorgyan, V. *Chem. Rev.* **2007**, *107*, 3117–3179. (c) Ma, S. *Pure Appl. Chem.* **2008**, *80*, 695–706. (d) Zhu, Z.-B.; Wei, Y.; Shi, M. *Chem. Soc. Rev.* **2011**, *40*, 5534–5563. (e) Miege, F.; Meyer, C.; Cossy, J. *Beilstein J. Org. Chem.* **2011**, *7*, 717–734. (f) Rubin, M.; Ryabchuk, P. G. *Chem. Heterocycl. Compd.* **2012**, *48*, 126–138.

(6) For selected examples, see: (a) Mushak, P.; Battiste, M. A. *J. Organomet. Chem.* **1969**, *17*, 46–48. (b) Battiste, M. A.; Friedrich, L. E.; Fiato, R. A. *Tetrahedron Lett.* **1975**, *1*, 45–48. (c) Donovan, B. T.; Hughes, R. P.; Spara, P. P.; Rheingold, A. L. *Organometallics* **1995**, *14*, 489–494. (d) Ma, S.; Zhang, J. *Angew. Chem., Int. Ed.* **2003**, *42*, 183–187. (e) Zhu, Z.-B.; Chen, K.; Wei, Y.; Shi, M. *Organometallics* **2011**, *30*, 627–632.

(7) For selected examples, see: (a) Lautens, M.; Meyer, C.; Lorenz, A. *J. Am. Chem. Soc.* **1996**, *118*, 10676–10677. (b) Rubina, M.; Rubin, M.; Gevorgyan, V. *J. Am. Chem. Soc.* **2002**, *124*, 11566–11567. (c) Rubina, M.; Rubin, M.; Gevorgyan, V. *J. Am. Chem. Soc.* **2004**, *126*, 3688–3689. (d) Simaan, S.; Masarwa, A.; Bertus, P.; Marek, I. *Angew. Chem., Int. Ed.* **2006**, *45*, 3963–3965. (e) Trofimov, A.; Rubina, M.; Rubin, M.; Gevorgyan, V. *J. Org. Chem.* **2007**, *72*, 8910–8920. (f) Sherrill, W. M.; Rubin, M. *J. Am. Chem. Soc.* **2008**, *130*, 13804–13809. (g) Alnasleh, B. K.; Sherrill, W. M.; Rubin, M. *Org. Lett.* **2008**, *10*, 3231–3234. (h) Phan, D. H. T.; Kou, K. G. M.; Dong, V. M. *J. Am. Chem. Soc.* **2010**, *132*, 16354–16355. (i) Tenaglia, A.; Jeune, K. L.; Giordano, L.; Buono, G. *Org. Lett.* **2011**, *13*, 636–639. (j) Matsuda, T.; Kirikae, H. *Organometallics* **2011**, *30*, 3923–3925. (k) Tarwade, V.; Selvaraj, R.; Fox, J. M. *J. Org. Chem.* **2012**, *77*, 9900–9904. (l) Nakano, T.; Endo, K.; Ukaji, Y. *Org. Lett.* **2014**, *16*, 1418–1421.

(8) (a) Hashmi, A. S. K.; Hutchings, G. J. *Angew. Chem., Int. Ed.* **2006**, *45*, 7896–7963. (b) Jiménez-Núñez, E.; Echavarren, A. M. *Chem. Commun.* **2007**, 333–346. (c) Fürstner, A.; Davies, P. W. *Angew. Chem., Int. Ed.* **2007**, *46*, 3410–3449. (d) Gorin, D. J.; Toste, F. D. *Nature* **2007**, *446*, 395–403. (e) Hashmi, A. S. K. *Chem. Rev.* **2007**, *107*, 3180–3211. (f) Gorin, D. J.; Sherry, B. D.; Toste, F. D. *Chem. Rev.* **2008**, *108*, 3351–3378. (g) Li, Z.; Brouwer, C.; He, C. *Chem. Rev.* **2008**, *108*, 3239–3265. (h) Abu Sohel, S. M.; Liu, R.-S. *Chem. Soc. Rev.* **2009**, *38*, 2269–2281. (i) Soriano, E.; Marco-Contelles, J. *Acc. Chem. Res.* **2009**, *42*, 1026–1036. (j) Sengupta, S.; Shi, X. *ChemCatChem* **2010**, *2*, 609–619. (k) Corma, A.; Leyva-Pérez, A.; Sabater, M. J. *Chem. Rev.* **2011**, *111*, 1657–1712. (l) Krause, N.; Winter, C. *Chem. Rev.* **2011**, *111*, 1994–2009. (m) Garayalde, D.; Nevado, C. *ACS Catal.* **2012**, *2*, 1462–1479. (n) Gulevich, A. V.; Dudnik, A. S.; Chernyak, N.; Gevorgyan, V. *Chem. Rev.* **2013**, *113*, 3084–3213. (o) Yang, W.; Hashmi, A. S. K. *Chem. Soc. Rev.* **2014**, *43*, 2941–2955. (p) Obradors, C.; Echavarren, A. M. *Acc. Chem. Res.* **2014**, *47*, 902–912. (q) Wang, Y.-M.; Lackner, A. D.; Toste, F. D. *Acc. Chem. Res.* **2014**, *47*, 889–901. (r) Fürstner, A. *Acc. Chem. Res.* **2014**, *47*, 925–938. (s) Hashmi, A. S. K. *Acc. Chem. Res.* **2014**, *47*, 864–876. (t) Friend, C. M.; Hashmi, A. S. K. *Acc. Chem. Res.* **2014**, *47*, 729–730.

(9) For selected examples, see: (a) Zhu, Z.-B.; Shi, M. *Chem.—Eur. J.* **2008**, *14*, 10219–10222. (b) Li, C.; Zeng, Y.; Wang, J. *Tetrahedron Lett.* **2009**, *50*, 2956–2959. (c) Seidel, G.; Mynott, R.; Fürstner, A. *Angew. Chem., Int. Ed.* **2009**, *48*, 2510–2513. (d) Seraya, E.; Slack, E.; Ariafard, A.; Yates, B. F.; Hyland, C. J. T. *Org. Lett.* **2010**, *12*, 4768–4771. (e) Miege, F.; Meyer, C.; Cossy, J. *Org. Lett.* **2010**, *12*, 4144–4147. (f) Li, J.; Sun, C.; Demerzhan, S.; Lee, D. *J. Am. Chem. Soc.* **2011**, *133*, 12964–12967. (g) Fang, R.; Yang, L.; Wang, Q. *Organometallics* **2012**, *31*, 4020–4030. (h) Liu, Y.; Zhang, D.; Bi, S. *Organometallics* **2012**, *31*, 4769–4778. (i) Hadfield, M. S.; Häller, L. J. L.; Lee, A.-L.; Macgregor, S. A.; O'Neill, J. A. T.; Watson, A. M. *Org.*

Biomol. Chem. **2012**, *10*, 4433−4440. (j) Hadfield, M. S.; Bauer, J. T.; Glen, P. E.; Lee, A.-L. *Org. Biomol. Chem.* **2010**, *8*, 4090−4095. (k) Young, P. C.; Hadfield, M. S.; Arrowsmith, L.; Macleod, K. M.; Mudd, R. J.; Jordan-Hore, J. A.; Lee, A.-L. *Org. Lett.* **2012**, *14*, 898−901. (l) Mudd, R. J.; Young, P. C.; Jordan-Hore, J. A.; Rosair, G. M.; Lee, A.-L. *J. Org. Chem.* **2012**, *77*, 7633−7639. (m) Hadfield, M. S.; Lee, A.-L. *Chem. Commun.* **2011**, *47*, 1333−1335. (n) Bauer, J. T.; Hadfield, M. S.; Lee, A.-L. *Chem. Commun.* **2008**, 6405−6407. (o) Rajabi, N. A.; Atashgah, M. J.; BabaAhmadi, R.; Hyland, C.; Ariafard, A. *J. Org. Chem.* **2013**, *78*, 9553−9559.

(10) (a) Cho, S. H.; Liebeskind, L. S. *J. Org. Chem.* **1987**, *52*, 2631−2634. (b) Nakamura, I.; Bajracharya, G. B.; Yamamoto, Y. *J. Org. Chem.* **2003**, *68*, 2297−2299. (c) Shibata, T.; Maekawa, S.; Tamura, K. *Heterocycles* **2008**, *76*, 1261−1270. (d) Li, C.; Zhang, H.; Zhang, Y.; Wang, J. *Org. Lett.* **2010**, *12*, 3082−3085. (e) Zhang, H.; Li, C.; Xie, G.; Wang, B.; Zhang, Y.; Wang, J. *J. Org. Chem.* **2014**, *79*, 6286−6293.

(11) (a) Nakamura, M.; Inoue, T.; Sato, A.; Nakamura, E. *Org. Lett.* **2000**, *2*, 2193. (b) Wang, Y.; Fordyce, E. A. F.; Chen, F. Y.; Lam, H. W. *Angew. Chem., Int. Ed.* **2008**, *47*, 7350−7353. (c) Li, C.; Zeng, Y.; Zhang, H.; Feng, J.; Zhang, Y.; Wang, J. *Angew. Chem., Int. Ed.* **2010**, *49*, 6413−6417. (d) Archambeau, A.; Miege, F.; Meyer, C.; Cossy, J. *Angew. Chem., Int. Ed.* **2012**, *51*, 11540−11544. (e) Didier, D.; Delaye, P.-O.; Simaan, M.; Island, B.; Eppe, G.; Eijsberg, H.; Kleiner, A.; Knochel, P.; Marek, I. *Chem.—Eur. J.* **2014**, *20*, 1038−1048. (f) Phun, L. H.; Aponte-Guzman, J.; France, S. *Angew. Chem., Int. Ed.* **2012**, *51*, 3198−3202. (g) Giudici, R. E.; Hoveyda, A. H. *J. Am. Chem. Soc.* **2007**, *129*, 3824−3825. (h) Shao, L.-X.; Zhang, Y.-P.; Qi, M.-H.; Shi, M. *Org. Lett.* **2007**, *9*, 117−120. (i) Zhou, Q.; Li, Y. *J. Am. Chem. Soc.* **2014**, *136*, 1505−1513.

(12) Marek, I.; Masarwa, A.; Delaye, P.-O.; Leibeling, M. *Angew. Chem., Int. Ed.* **2014**, DOI: 10.1002/anie.201405067.

(13) Ma, S.; Zhang, J. *J. Am. Chem. Soc.* **2003**, *125*, 12386−12387.

(14) For related works by the S. Ma group, see: (a) Ma, S.; Lu, L.; Zhang, J. *J. Am. Chem. Soc.* **2004**, *126*, 9645−9660. (b) Chen, J.; Ni, S.; Ma, S. *Synlett* **2011**, 931−934.

(15) Padwa, A.; Kassir, J. M.; Xu, S. L. *J. Org. Chem.* **1991**, *56*, 6971−6972.

(16) For related works by the Padwa group, see: (a) Padwa, A.; Kassir, J. M.; Xu, S. L. *J. Org. Chem.* **1997**, *62*, 1642−1652. (b) Padwa, A.; Austin, D. J.; Gareau, Y.; Kassir, J. M.; Xu, S. L. *J. Am. Chem. Soc.* **1993**, *115*, 2637−2647. (c) Padwa, A.; Xu, S. L. *J. Am. Chem. Soc.* **1992**, *114*, 5881−5882. (d) Padwa, A.; Austin, D. J.; Xu, S. L. *J. Org. Chem.* **1992**, *57*, 1330−1331.

(17) Chuprakov, S.; Gevorgyan, V. *Org. Lett.* **2007**, *9*, 4463−4466.

(18) Chen, J.; Ma, S. *Chem. -Asian J.* **2010**, *5*, 2415−2421.

(19) Gong, J.; Zhao, Z.; Zhang, F.; Wu, S.; Yan, G.; Quan, Y.; Ma, B. *Org. Lett.* **2014**, *16*, 5524−5527.

(20) For selected recent examples, see: (a) Sromek, A. W.; Rubina, M.; Gevorgyan, V. *J. Am. Chem. Soc.* **2005**, *127*, 10500−10501. (b) Dudnik, A. S.; Sromek, A. W.; Rubina, M.; Kim, J. T.; Kel'in, A. V.; Gevorgyan, V. *J. Am. Chem. Soc.* **2008**, *130*, 1440−1452. (c) Xia, Y.; Dudnik, A. S.; Gevorgyan, V.; Li, Y. *J. Am. Chem. Soc.* **2008**, *130*, 6940−6941. (d) Dudnik, A. S.; Xia, Y.; Li, Y.; Gevorgyan, V. *J. Am. Chem. Soc.* **2010**, *132*, 7645−7655. (e) Shiroodi, R. K.; Koleda, O.; Gevorgyan, V. *J. Am. Chem. Soc.* **2014**, *136*, 13146−13149. (f) Lu, B.; Wu, J.; Yoshikai, N. *J. Am. Chem. Soc.* **2014**, *136*, 11598−11601. (g) Ma, Y.; Zhang, S.; Yang, S.; Song, F.; You, J. *Angew. Chem., Int. Ed.* **2014**, *53*, 7870−7874. (h) Zhou, L.; Zhang, M.; Li, W.; Zhang, J. *Angew. Chem., Int. Ed.* **2014**, *53*, 6542−6545. (i) Pennell, M. N.; Foster, R. W.; Turner, P. G.; Hailes, H. C.; Tame, C. J.; Sheppard, T. D. *Chem. Commun.* **2014**, *50*, 1302−1304. (j) Nitsch, D.; Bach, T. *J. Org. Chem.* **2014**, *79*, 6372−6379. (k) Mal, K.; Sharma, A.; Das, I. *Chem.—Eur. J.* **2014**, *20*, 11932−11945. (l) Palisse, A.; Kirsch, S. F. *Eur. J. Org. Chem.* **2014**, 7095−7098. (m) Xia, L.; Lee, Y. R. *Eur. J. Org. Chem.* **2014**, 3430−3442. (n) Xia, Y.; Xia, Y.; Ge, R.; Liu, Z.; Xiao, Q.; Zhang, Y.; Wang, J. *Angew. Chem., Int. Ed.* **2014**, *53*, 3917−3921. (o) Song, C.; Ju, L.; Wang, M.; Liu, P.; Zhang, Y.; Wang, J.; Xu, Z. *Chem.—Eur. J.* **2013**, *19*, 3584−3589. (p) Jiang, H.; Yin, M.; Li, Y.; Liu, B.; Zhao, J.; Wu, W. *Chem. Commun.* **2014**, *50*, 2037−2039.

(q) Cao, H.; Jiang, H.; Yao, W.; Liu, X. *Org. Lett.* **2009**, *11*, 1931−1933. (r) Liu, W.; Jiang, H.; Zhang, M.; Qi, C. *J. Org. Chem.* **2010**, *75*, 966−968. (s) Jiang, H.; Yao, W.; Cao, H.; Huang, H.; Cao, D. *J. Org. Chem.* **2010**, *75*, 5347−5350. (t) Zheng, M.; Huang, L.; Wu, W.; Jiang, H. *Org. Lett.* **2013**, *15*, 1838−1841. (u) Jiang, H.; Pan, X.; Huang, L.; Zhao, J.; Shi, D. *Chem. Commun.* **2012**, *48*, 4698−4700. (v) Wang, T.; Shi, S.; Hansmann, M. M.; Rettenmeier, E.; Rudolph, M.; Hashmi, A. S. K. *Angew. Chem., Int. Ed.* **2014**, *53*, 3715−3719.

(21) For selected recent examples, see: (a) Michlik, S.; Kempe, R. *Nat. Chem.* **2013**, *5*, 140−144. (b) Zhang, M.; Neumann, H.; Beller, M. *Angew. Chem., Int. Ed.* **2013**, *52*, 597−601. (c) Srimani, D.; Ben-David, Y.; Milstein, D. *Angew. Chem., Int. Ed.* **2013**, *52*, 4012−4015. (d) Zhang, M.; Fang, X.; Neumann, H.; Beller, M. *J. Am. Chem. Soc.* **2013**, *135*, 11384−11388. (e) Xuan, J.; Xia, X.-D.; Zeng, T.-T.; Feng, Z.-J.; Chen, J.-R.; Lu, L.-Q.; Xiao, W.-J. *Angew. Chem., Int. Ed.* **2014**, *53*, 5653−5656. (f) Wu, T.; Pan, L.; Xu, X.; Liu, Q. *Chem. Commun.* **2014**, *50*, 1797−1800. (g) Meng, X.; Liao, P.; Liu, J.; Bi, X. *Chem. Commun.* **2014**, *50*, 11837−11839. (h) Debrouwer, W.; Heugebaert, T. S. A.; Stevens, C. V. *J. Org. Chem.* **2014**, *79*, 4322−4331. (i) Yu, Y.; Wang, C.; He, X.; Yao, X.; Zu, L. *Org. Lett.* **2014**, *16*, 3580−3583. (j) Ueda, H.; Yamaguchi, M.; Kameya, H.; Sugimoto, K.; Tokuyama, H. *Org. Lett.* **2014**, *16*, 4948−4951.

(22) For examples of halometalation in other systems, see: (a) Lu, X. *Handbook of Organopalladium Chemistry for Organic Synthesis*; Negishi, E., Ed.; Wiley-Interscience: New York, 2002; Vol. 2, pp 2267−2288. (b) Wu, W.; Jiang, H. *Acc. Chem. Res.* **2012**, *45*, 1736−1748. (c) Huang, L.; Wang, Q.; Liu, X.; Jiang, H. *Angew. Chem., Int. Ed.* **2012**, *51*, 5696−5700. (d) Huang, J.; Zhou, L.; Jiang, H. *Angew. Chem., Int. Ed.* **2006**, *45*, 1945−1949. (e) Zhang, H.-P.; Yu, S.-C.; Liang, Y.; Peng, P.; Tang, B.-X.; Li, J.-H. *Synlett* **2011**, 982−988. (f) Huang, X.-C.; Wang, F.; Liang, Y.; Li, J.-H. *Org. Lett.* **2009**, *11*, 1139−1142.

(23) For examples of theoretical studies on $PdCl_2$ catalysis, see: (a) Lan, Y.; Deng, L.; Liu, J.; Wang, C.; Wiest, O.; Yang, Z.; Wu, Y.-D. *J. Org. Chem.* **2009**, *74*, 5049−5058. (b) Ramana, C. V.; Patel, P.; Vanka, K.; Miao, B.; Degterev, A. *Eur. J. Org. Chem.* **2010**, 5955−5966. (c) Kovács, G.; Stirling, A.; Lledós, A.; Ujaque, G. *Chem.—Eur. J.* **2012**, *18*, 5612−5619.

(24) For examples of theoretical studies on CuI catalysis, see: (a) Xiao, Q.; Ling, L.; Ye, F.; Tan, R.; Tian, L.; Zhang, Y.; Li, Y.; Wang, J. *J. Org. Chem.* **2013**, *78*, 3879−3885. (b) Wang, P.-y.; Li, L.-c.; Yang, C.; Li, Y.-r. *J. Phys. Chem. A* **2008**, *112*, 435−440. (c) Yu, H.-Z.; Jiang, Y.-Y.; Fu, Y.; Liu, L. *J. Am. Chem. Soc.* **2010**, *132*, 18078−18091. (d) Jones, G. O.; Liu, P.; Houk, K. N.; Buchwald, S. L. *J. Am. Chem. Soc.* **2010**, *132*, 6205−6213. (e) Zhang, S.-L.; Bie, W.-F.; Huang, L. *Organometallics* **2014**, *33*, 5263−5271. (f) Li, J.; Gu, H.; Wu, C.; Du, L. *Dalton Trans.* **2014**, *43*, 16769−16779. (g) Wang, M.; Fan, T.; Lin, Z. *Organometallics* **2012**, *31*, 560−569.

(25) Frisch, M. J.; Trucks, G. W.; Schlegel, H. B.; Scuseria, G. E.; Robb, M. A.; Cheeseman, J. R.; Scalmani, G.; Barone, V.; Mennucci, B.; Petersson, G. A.; Nakatsuji, H.; Caricato, M.; Li, X.; Hratchian, H. P.; Izmaylov, A. F.; Bloino, J.; Zheng, G.; Sonnenberg, J. L.; Hada, M.; Ehara, M.; Toyota, K.; Fukuda, R.; Hasegawa, J.; Ishida, M.; Nakajima, T.; Honda, Y.; Kitao, O.; Nakai, H.; Vreven, T.; Montgomery, J. A., Jr.; Peralta, J. E.; Ogliaro, F.; Bearpark, M.; Heyd, J. J.; Brothers, E.; Kudin, K. N.; Staroverov, V. N.; Kobayashi, R.; Normand, J.; Raghavachari, K.; Rendell, A.; Burant, J. C.; Iyengar, S. S.; Tomasi, J.; Cossi, M.; Rega, N.; Millam, N. J.; Klene, M.; Knox, J. E.; Cross, J. B.; Bakken, V.; Adamo, C.; Jaramillo, J.; Gomperts, R.; Stratmann, R. E.; Yazyev, O.; Austin, A. J.; Cammi, R.; Pomelli, C.; Ochterski, J. W.; Martin, R. L.; Morokuma, K.; Zakrzewski, V. G.; Voth, G. A.; Salvador, P.; Dannenberg, J. J.; Dapprich, S.; Daniels, A. D.; Farkas, Ö.; Foresman, J. B.; Ortiz, J. V.; Cioslowski, J.; Fox, D. J. *Gaussian 09*, Revision A.02; Gaussian, Inc.: Wallingford, CT, 2009.

(26) (a) Lee, C. T.; Yang, W. T.; Parr, R. G. *Phys. Rev. B* **1988**, *37*, 785−789. (b) Miehlich, B.; Savin, A.; Stoll, H.; Preuss, H. *Chem. Phys. Lett.* **1989**, *157*, 200−206. (c) Becke, A. D. *J. Chem. Phys.* **1993**, *98*, 5648−5652.

(27) (a) Ditchfield, R.; Hehre, W. J.; Pople, J. A. *J. Chem. Phys.* **1971**, *54*, 724−728. (b) Hehre, W. J.; Pople, J. A. *J. Chem. Phys.* **1972**, *56*,

4233−4234. (c) Hehre, W. J.; Ditchfield, R.; Pople, J. A. *J. Chem. Phys.* **1972**, *56*, 2257−2261. (d) Binkley, J. S.; Pople, J. A. *J. Chem. Phys.* **1977**, *66*, 879−880.

(28) (a) Andrae, D.; Haussermann, U.; Dolg, M.; Stoll, H.; Preuss, H. *Theor. Chim. Acta* **1990**, *77*, 123−141. (b) Leininger, T.; Nicklass, A.; Stoll, H.; Dolg, M.; Schwerdtfeger, P. *J. Chem. Phys.* **1996**, *105*, 1052−1059.

(29) (a) Fukui, K. *J. Phys. Chem.* **1970**, *74*, 4161−4163. (b) Fukui, K. *Acc. Chem. Res.* **1981**, *14*, 363−368.

(30) Tomasi, J.; Persico, M. *Chem. Rev.* **1994**, *94*, 2027−2094.

(31) (a) Liu, Y.; Ma, S. *Org. Lett.* **2012**, *14*, 720−723. (b) Ni, S.; Chen, J.; Ma, S. *Org. Lett.* **2013**, *15*, 3290−3293. (c) Ma, S.; Zhang, J.; Cai, Y.; Lu, L. *J. Am. Chem. Soc.* **2003**, *125*, 13954−13955. (d) Ma, S.; Zhang, J.; Lu, L.; Jin, X.; Cai, Y.; Hou, H. *Chem. Commun.* **2005**, 909−911. (e) Chen, J.; Ma, S. *J. Org. Chem.* **2009**, *74*, 5595−5598. (f) Liu, Y.; Yu, Q.; Ma, S. *Eur. J. Org. Chem.* **2013**, 3033−3040.

(32) Kobayashi, S.; Busujima, T.; Nagayama, S. *Chem.—Eur. J.* **2000**, *6*, 3491−3494.

(33) (a) Ess, D. H.; Houk, K. N. *J. Am. Chem. Soc.* **2007**, *129*, 10646−10647. (b) Legault, C. Y.; Garcia, Y.; Merlic, C. A.; Houk, K. N. *J. Am. Chem. Soc.* **2007**, *129*, 12664−12665. (c) Ess, D. H.; Houk, K. N. *J. Am. Chem. Soc.* **2008**, *130*, 10187−10198. (d) Gorelsky, S. I.; Lapointe, D.; Fagnou, K. *J. Am. Chem. Soc.* **2008**, *130*, 10848−10849. (e) Hayden, A. E.; Houk, K. N. *J. Am. Chem. Soc.* **2009**, *131*, 4084−4089. (f) Schoenebeck, F.; Ess, D. H.; Jones, G. O.; Houk, K. N. *J. Am. Chem. Soc.* **2009**, *131*, 8121−8133. (g) Liang, Y.; Mackey, J. L.; Lopez, S. A.; Liu, F.; Houk, K. N. *J. Am. Chem. Soc.* **2012**, *134*, 17904−17907. (h) Usharani, D.; Lacy, D. C.; Borovik, A. S.; Shaik, S. *J. Am. Chem. Soc.* **2013**, *135*, 17090−17104. (i) Hong, X.; Liang, Y.; Houk, K. N. *J. Am. Chem. Soc.* **2014**, *136*, 2017−2025. (j) Liu, F.; Liang, Y.; Houk, K. N. *J. Am. Chem. Soc.* **2014**, *136*, 11483−11493. (k) Green, A. G.; Liu, P.; Merlic, C. A.; Houk, K. N. *J. Am. Chem. Soc.* **2014**, *136*, 4575−4583. (l) Liu, S.; Qi, X.; Lan, Y. *J. Phys. Chem. A* **2014**, *118*, 2638−2645. (m) Hong, X.; Liang, Y.; Brewer, M.; Houk, K. N. *Org. Lett.* **2014**, *16*, 4260−4263.

(34) (a) van Zeist, W.-J.; Bickelhaupt, F. M. *Org. Biomol. Chem.* **2010**, *8*, 3118−3127. (b) Fernández, I.; Cossío, F. P.; Bickelhaupt, F. M. *J. Org. Chem.* **2011**, *76*, 2310−2314. (c) Fernández, I.; Bickelhaupt, F. M. *J. Comput. Chem.* **2012**, *33*, 509−516. (d) Fernández, I.; Wolters, L. P.; Bickelhaupt, F. M. *J. Comput. Chem.* **2014**, *35*, 2140−2145.

(35) Fernández, I.; Bickelhaupt, F. M. *Chem. Soc. Rev.* **2014**, *43*, 4953−4967.

(36) The standard bond dissociation energies predicted by B3LYP/6-311++G(2d,p) calculations for the C^1-C^3 and C^2-C^3 σ bonds in **1a** are 21.1 and 32.3 kcal/mol, respectively.